Published in final edited form as:
Comput Biomed Res. 1967 July ; 1(2): 124–138.

A Steady-State Transfer Function Analysis of Portions of the Circulatory System Using Indicator Dilution Techniques*

Craig M. Coulam†,
Department of Biophysics and Bioengineering, University of Utah and Latter-day Saints Hospital, Salt Lake City, Utah 84103

Homer R. Warner,
Department of Biophysics and Bioengineering, University of Utah and Latter-day Saints Hospital, Salt Lake City, Utah 84103

Hiram W. Marshall, and
Holy Cross Hospital and University of Utah Medical School, Salt Lake City, Utah 84102

James B. Bassingthwaighte
Department of Physiology, Mayo Graduate School of Medicine, Rochester, Minnesota 55901

Abstract

A digital computer program has been developed whereby the distribution of dye-particle transit times across circulatory pathways can be found from recordings of upstream and downstream indicator-dilution curves. This distribution or transfer function is computed from Fourier-series representations of the upstream and downstream indicator curves and makes possible, for the first time, the calculation of transit-time distributions independent of the effects of recirculating dye. Since a discontinuity is introduced into the tails of the upstream and downstream curves at the end of sampling, the method requires an iterative approach in the termination of the upstream and downstream curves. The accuracy of the calculated distribution pattern is determined by comparison of the recorded downstream curve with the results of the convolution of the recorded upstream curve and computed transfer function. Effects of noise, bandwidth and sampling rate have been investigated through the use of analog computer models of the circulatory pathways. These studies show that the transfer-function description is limited by the bandwidth of the upstream (input) curve. Noise, or variations in magnitude and phase angle of input- and output-curve frequencies, tends to introduce oscillations into the time-domain representation of the transfer function as does the use of too few frequencies. This means that in biological systems the upstream sampling site must be relatively close to the dye injection site if the input and output sampling sites are close together. Circulatory transfer functions have been obtained from dogs across their lower extremity, renal and systemic circulations before, during and following moderate exercise (walking on treadmill at two miles per hour for four minutes).

I. Introduction

Indicator-dilution curves play an important role in the study of the circulation both in the calculation of cardiac output and in the study of downstream dispersion patterns following upstream injections. In other application, however, recirculating indicator often limits the

*This work was supported by National Institutes of Health Fellowship No. F1-GM-16, 769, Research Grant No. 5 P07 FR-00012 and Research Grant No. HE 04664.

†This is an essential portion of a thesis submitted to the Department of Biophysics & Bioengineering, University of Utah, in partial fulfillment of the requirements of a Doctor of Philosophy Degree.

amount of information that can be derived. For example, the calculation of cardiac output from a dilution-curve recording requires the separation of that part of the curve due to particles passing the recording site for the first time from that due to indicator recirculating past that site. This time separation is generally made using an exponential extrapolation of the initial downslope of the dilution curve (as described by Hamilton[1]), when the distribution of transit times between the injection and sampling site is small compared to the appearance time of the recirculating dye particles. When this distribution criterion is not met, recirculation can be confused with initial circulation in such a way that separation by exponential extrapolation methods is no longer possible.

The most interesting transit-time distributions, however, are often those which contain multiple peaks.[2] Such distributions represent the mixing properties of the vascular system and result from the addition of flowstreams coming from vascular beds having different dispersion and transit-time properties. In a situation such as this, conventional methods of removing recirculation are not applicable.[3] This paper presents a method for obtaining the distribution of transit times through a vascular bed independent of any assumptions concerning recirculating dye particles and independent of the characteristics of the sampling/detecting system used to measure the indicator-dilution curves.

II. Theory

The dispersion of an indicator across a vascular bed is the result of indicator particles traversing vascular pathways which require different passage or transit times.[4] This distribution of indicator-particle transit times is what would be seen in the venous system following a rapid upstream or arterial indicator injection were there no recirculation of indicator present. Thus the distribution of transit times is the vascular system's unit impulse response or its time-domain transfer function.

To calculate this distribution of particle transit times, independent of recirculation, a simplified model of the vascular system is proposed in Figure 1. This model shows a generalized flow diagram where one vascular bed, whose distribution properties are to be determined, is represented by Box A and the other vascular beds by Box B. Box A represents the forward loop of a general feedback block diagram and Box B the recirculation or feedback loop. The use of block diagram analysis techniques may be used when the dispersion properties of the vascular system can be shown to be linear and stationary (i.e., obey the superposition principle).[5] To a first approximation linearity and stationarity may be tested by making a comparison between the time-course of indicator concentrations resulting from injections of X mgm and 2X mgm of indicator material.[6] If the contours of the resulting time-concentration curves are identical, the peaks of the curve occur at the same time and the amplitude of one curve is twice the other, linearity and stationarity may be assumed. Deviations from the ideal linear and stationary state do occur under experimental conditions, of course, and will be discussed in a later section of this paper.

To find the transfer function or distribution of indicator transit times of Box A, the input curve $f(t)$ is transformed into its Laplace-domain equivalent $F(s)$, and the downstream curve $g(t)$ into its equivalent $G(s)$. The transfer function $H(s)$ is thus defined as $G(s)/F(s)$. However, if we assume steady state conditions and consider only discrete upstream- and downstream-curve representations (as result from digital sampling), then we can make the substitution $s = 2\pi n/P$ where s is the Laplacian variable, n is the harmonic frequency index and P is the period or total number of sampling points for each curve. In this situation, $f(t)$ may now be transformed into $F(n)$ and $g(t)$ into $G(n)$ by using a Fourier-series transformation instead of a Laplace transformation since $f(t)$ and $g(t)$ are now discrete functions.[7] Equations (1)–(4) describe the transformation of $f(t)$ into $F(n)$ and Equations 5–9

describe the calculation of the frequency-domain transfer function $H(n)$ and subsequent generation of its time-domain analog, $h(t)$. In these equations, $a(n)_F$ and $b(n)_F$ represent the upstream amplitude coefficients for the cosine and sine terms, respectively, $F(n)$ is the vector sum of $a(n)_F$ and $b(n)_F$ and $\phi(n)_F$ is the resulting phase angle.

For the special case where injected indicator passes the recording site only once (open-loop conditions), all of the injected dye would be expected to pass through Box A in some finite time. In the more general closed-loop case, however, the problem becomes more complex since both injected and recirculating indicator is recorded going into Box A and, therefore, must also be recorded coming out. This condition is not fulfilled when parallel sampling of the upstream and downstream signals is terminated at exactly the same time since more dye will have been recorded going into the bed than will have been recorded coming out due to the finite transit-time required by the dye particles. This type of recording error does occur and it is thus necessary to add to the tail of the downstream curve the missing information. At the same time, it is desirable to terminate both the upstream and downstream curve with some smooth function in order to eliminate any high-frequency harmonic terms which are normally introduced when a step discontinuity is used as the curve termination. To accomplish this termination procedure, the upstream curve is returned to a zero concentration using the function $f_1(t)$ given by Eqs. (10) and (11). In these equations, σ and t_0 characterize a normal Gaussian distribution. Next, the downstream curve is terminated by the function $f_3(t)$ given by Eq. (14). This terminating curve, $f_3(t)$, is the result of the convolution of $f_1(t)$ and $f_2(t)$ where $f_2(t)$ is an assumed vascular-bed transfer function defined by Eqs. (12) and (13) and accounts for the transit time and dispersion of dye particles occurring in the vascular bed at the end of sampling.

Figure 2 shows a representation of the terminated upstream and downstream curves. Since these curves are both mathematically and physically complete representations of the vascular system's upstream and downstream curves, Eqs. (1)–(9) can now be used to calculate the vascular bed's transfer function, $h(t)$. However, since it was necessary to assume a transfer function $h_1(t)$ in order to terminate $g(t)$, we can now terminate the downstream curve with a more exact transfer function representation, $h(t)$. Thus the repetitive use of Eqs. (1)–(14), where the latest $h(t)$ is always substituted for $h_1(t)$ in Eq. (12), allows for convergence on to the optimal transfer function in an iterative manner.

Fourier Series

$$a(n)_F = \frac{2}{P}\int_{-P/2}^{P/2} f(t)\cos\frac{2\pi n}{P}\,t\,dt \quad n=0, 1, 2, \_\_\_, N. \tag{1}$$

$$b(n)_F = \frac{2}{P}\int_{P/2}^{P/2} f(t)\sin\frac{2\pi n}{P}\,t\,dt \quad n=1, 2, \_\_\_\_\_, N \tag{2}$$

where P = period or number of data points and $b(o) = 0$,

$$F(n)=[a(n)^2+b(n)^2]^{1/2} \tag{3}$$

$$\varphi(n)_F = \tan^{-1}\frac{b(n)}{a(n)}. \tag{4}$$

Transfer-Function Computation

$$H(n) = \frac{G(n)}{F(n)}, \tag{5}$$

$$\varphi(n)_H = \varphi(n)_G - \varphi(n)_F, \tag{6}$$

$$a(n)_H = H(n)\cos\varphi(n)_H, \tag{7}$$

$$b(n)_H = H(n)\sin\varphi(n)_H, \tag{8}$$

$$h(t) = \frac{a(o)}{2} + \sum_{n=1}^{N}\left[a(n)_H \cos\frac{2\pi n}{P}t + b(n)_H \sin\frac{2\pi n}{P}t\right], \tag{9}$$

where N = total number of coefficients used for forming curve.

Tail Extrapolation

$$n(t) = \frac{1}{\sigma(2\pi)^{1/2}}\exp\left(-\frac{(t-t_0)^2}{2\sigma^2}\right), \tag{10}$$

$$f_1(t) = K_1\left[1 - \int_0^P n(t)\,dt\right], \tag{11}$$

$$h_1(t) = n(t) - \tau h_1'(t), \tag{12}$$

$$f_2(t) = 1 - \int_0^P h_1(t)\,dt, \tag{13}$$

$$f_3(t) = \int^P f_1(\tau)\, f_2(t-\tau)\,d\tau, \tag{14}$$

III. Tests of the Method

To determine how accurately the transfer function can be recovered, even in the presence of recirculating dye, a model of a linear three-pathway mixing process was programmed on the analog computer (Fig. 3). This analog model simulates the conditions which parallel pathways may have on the indicator dispersion process by assuming that each pathway behaves as a delayed, low-pass filter. Therefore, each box in Fig. 3 represents either a filter circuit characterized by a break-frequency (tau) or a variable phase delay. The true transfer function of the model can be recorded directly at $g(t)$ when the input, $i(t)$, is a unit impulse and there is no recirculation (feedback) present. Thus the accuracy of the digital computer method which is used for calculating the transfer function of the closed-loop system from recordings of the input and output curves may be investigated through a comparison of the calculated $h(t)$ and the recorded impulse response of the model.

Figure 4 shows the recording of an input curve $f(t)$, output curve $g(t)$, and unit impulse response or transfer function of the upper pathway of the model of Fig. 3 in which no recirculation was present (pathways *b* and *c* open). Superimposed on the recorded transfer function is the computed transfer function and superimposed on the output curve is the computed output curve found by convolution of $f(t)$ with $h(t)$. From this drawing it can be seen that, with no recirculation, the recorded and computed transfer functions are nearly identical as are the recorded and computed output curves. Figure 5 shows the results of similar calculations made from the closed-loop model (pathway *b* open, *c* closed). Again recorded and computed transfer functions (lower frame) and output curves (upper frame) agree favorably; however, the computed transfer function of Fig. 5 does show a slightly greater deviation from its true wave-form than does the computed transfer function of Fig. 4. This error may come from the fact that the true terminating tail of $g(t)$ may not have been found by the end of the computational process which here included only three iterations.

Since the results of Figs. 4 and 5 show that it is possible to calculate a system's unit impulse response from recordings of its input and output signals, with or without recirculation effects and assuming only steady state conditions, it then becomes desirable to investigate further conditions which must be met in order to characterize quantitatively the transfer-function representation. The model of Fig. 3 will again furnish the necessary data.

A. Harmonic Content of the Transfer Function

If a known transfer function contains N harmonic components, then to give an adequate description of the transfer function in the time-domain, N harmonic components must be known in the transfer function's Fourier-series representation. Since the transfer function is calculated from a recording of a system's input and output signals, then it is necessary that the input signal contain a minimum of N significant terms. Figure 6 shows what happens when this criteria is not met. The lower frame depicts the situation in which both the input signal (with recirculation) and the known transfer function contain 40 significant harmonic components. Here an adequate time-domain transfer function has been calculated from the input and the output signals. In the upper frame, however, the input signal contains only 30 frequency terms. In this case only 30 of the actual 40 transfer-function harmonic terms may be calculated from the input and output curves. The loss of the last ten high-frequency components thus results in a time-domain transfer function which contains tail oscillations. These oscillations are known as Gibb's phenomena and may be attenuated, to some degree, through the use of Lanczos' sigma factors. It is more desirable, however, to guarantee the presence of the required harmonic terms in the upstream curve by injecting the indicator as rapidly as possible without creating hemolysis and by locating the upstream sampling site as close to the injection site as possible.

B. Convolution Routine

The precision (in contrast to the completeness) of an unknown vascular bed's transfer function description may be assessed by comparing the recorded downstream curve with the results of the convolution of the calculated transfer function and the recorded upstream curve. In this study a correlation coefficient of 0.997 or greater was used to indicate that sufficient precision in calculating the transfer function had been achieved. The difference between completeness and the precision of a transfer-function calculation under a variety of transfer-function conditions is shown in Figs. 4, 5, and 6. Even though good correlations between computed and recorded output curves may be obtained, it is apparent that the true transfer function may not have been determined. This points out the fact that the process of convolution merely relates an input curve to an output curve and says nothing as to whether all of the frequencies needed to adequately represent the transfer function have been defined.

C. Signal Noise and Sampling Theory

The effect of noise (noise being defined here as any unwanted signal such as cardiac cycle variations, respiratory cycle variations, instrumentation noise, etc.) is to create deviations from the true amplitude and phase characteristics of the input- and output-curve frequency-domain representations. True noise (i.e., white noise) in general results in small random variations, in signal amplitude, and phase representations around their exact value, and, therefore, generates variations in the transfer-function harmonic-term computations. However, essentially all major frequency-domain variation comes from aliasing[8] effects which are generated by the sampling of indicator curves at a rate which is less than noise frequencies contained in the dilution curve signal. Aliasing, in general, reflects high-frequency signal energy into low-frequency bands and thus adds distortion to the already existing signal harmonic terms. The use of presampling analog filtering generally will completely remove these effects if care is taken to insure adequate attenuation of noise-frequency terms (i.e., the use of a low-pass, sharp-cutoff analog filter). Once aliasing effects have occurred, however, no amount of digital filtering will remove this added distortion without also creating additional distortion to the desired indicator-curve frequency content. When aliasing effects do occur, the variations imposed upon the upstream and downstream frequency spectrums may be such that large error can be generated in $H(n)$ when dividing $G(n)$ by $F(n)$ as required by Eq. (5). This type of error generation will occur when the frequency-domain distortion is different for the upstream and the downstream curve.

Figure 7 shows the situation where a dominant, high-frequency signal (signal-to-noise ratio of 10) has been added to both the upstream and downstream curves of the analog computer model. The digital sampling rate of the upstream- and downstream-curve signals was made at a rate which was less than that of the added frequency, thus, guaranteeing aliasing effects. It can be seen from this figure that, even though the transfer function appears to be adequately defined, its convolution with the upstream curve does not accurately predict the recorded downstream curve. In this situation the process of convolution and comparison of downstream signals becomes the sole check on the precision and the completeness of the calculated transfer function.

D. Effects of the Sampling System

To record an indicator dilution curve it is necessary to insert into the vascular system at some designated site some means of sampling the dye–blood mixture. This is generally done by placing a catheter into the bloodstream and withdrawing the blood–dye mixture through this channel and into either an oximeter cuvette or a densitometer, which, in turn, gives an electrical signal proportional to the concentration of the indicator in the blood. However, as the blood is pulled through the catheter, the distribution of indicator concentration is

changed by the variation in flow velocity across the catheter profile. This change in indicator concentration, as it traverses the sampling system, is referred to as catheter distortion.

One advantage of the method here described is that the calculated transfer function of the vascular system is theoretically independent of the recording apparatus if identical sampling equipment is used. This can be shown as follows: Let $T_f(n)$ and $T_g(n)$ represent the upstream- and downstream-catheter harmonic frequency properties respectively and $F_t(n)$ and $G_t(n)$ the indicator time concentration curves seen at the upstream- and downstream-catheter tips respectively. The upstream and downstream curves that are actually recorded or detected by the oximeter cuvettes are then

$$F(n)=F_t(n)T_f(n), \tag{15}$$

and

$$G(n)=G_t(n)T_g(n). \tag{16}$$

Thus, the vascular-bed transfer function is

$$H(n)=\frac{G(n)}{F(n)}=\frac{G_t(n)T_g(n)}{F_t(n)T_f(n)} \tag{17}$$

or

$$H(n)=G_t(n)/F_t(n) \tag{18}$$

when $T_g(n) = T_f(n)$. In actual experiments, however, $T_g(n)$ is never quite identical to $T_f(n)$ because $T_g(n)$ and $T_f(n)$ are dependent upon curves and bends in the catheter geometry.[9]

In summary, this section has presented the mathematics and necessary criteria for obtaining a time and frequency-domain representation of the forward-loop transfer function in the presence of a feedback signal. The conditions of the model were linearity and stationarity and with the added assumption of steady-state conditions, Fourier-series transformations were used. Problems pertaining to end-of-sampling effects, transfer-function harmonic-term content, convolution-routine limitations, sampling, noise, aliasing effects, and catheter-distortion conditions were investigated.

IV. Experimental Methods

Indicator-dilution curves were obtained from mongrel dogs using no 6F, 100-cm teflon cardiac catheters which were positioned, under fluoroscopic control, in the left ventricle for indicator injection (cardiogreen dye), in the ascending aorta for upstream (input) sampling, and in the pulmonary artery (PA), inferior vena cava (IVC, cephalad to the iliac bifurcation), and renal vein for downstream (output) sampling. Following a 5-mg dye injection, blood–dye mixtures were simultaneously withdrawn through the upstream and two downstream catheters at 9 ml/min into Wood oximeter cuvettes whose electrical outputs went directly to an analog-to-digital converter (A-to-D). The time–concentration curves were sampled four

times per second for 120 seconds and stored on digital magnetic tape. Following each injection, transfer functions between upstream and downstream sites were immediately calculated thus giving the investigator chronological information as to the state or condition of the vascular bed under study or to possible movements of the catheter tip's anatomical location.

Figure 8 shows the upstream aortic curve, the downstream renal-vein curve, the computed downstream curve and the calculated transfer function. From this we see that the correlation (r = 0.998) between the recorded and computed downstream curves is quite good even though the transfer function contains some oscillations in its tail portions. These oscillations are probably not physiologically significant, but are a result of an incomplete harmonic description of the renal vascular bed as discussed in the Theory section. It can be inferred from this renal transfer function, however, that the blood-transit time is extremely rapid ($\bar{t}$ = 7.5 seconds) and has a narrow dispersion pattern.

Figure 9 shows a four-frame representation of the effects of exercise on the lower-extremity blood circulation (IVC) and its relationship to the total systemic blood distribution (PA). The upper left frame depicts the control state. Here the large, narrow peak on the pulmonary-artery curve represents the effects of renal blood passage (and possibly some coronary blood flow), while the rest of the curve shows the dispersion effects of the remainder of the systemic vascular bed. The IVC curve contains a delayed appearance time and a broad dispersion pattern which depicts a slow blood-transit time. The upper right frame shows data representing the exercise state and was obtained from dye curves recorded during the last two minutes of a four-minute period when the dog was walking on a slightly inclined treadmill at two miles per hour. Note in this frame that the lower-extremity (IVC) blood-transit time and dispersion is greatly decreased and now approaches that of the renal component of the PA curve. In fact, the entire PA curve has shifted toward the renal component which indicates a general decrease in total systemic blood-transit time ($\bar{t}$ = 14.4 sec compared to t = 27.3 sec for the control state). The lower two frames show PA and IVC curves ten and 20 min post-exercise. Note here that the PA curve is beginning to return to its control-state recording but has not yet obtained it by 20 minutes post-exercise. In some dogs the control-state distribution pattern would not be reached for as long as one hour following exercise even though the animal's cardiac output (computed from the aortic curve using a Stewart–Hamilton extrapolation) was back to normal within three minutes after exercise. Thus, by studying transfer functions in the time domain, the effects of drugs and/or physiological stresses on the vascular system can be determined independent of the effects of recirculation.

References

1. Moore JW, Kinsman JM, Hamilton WF, Spurling RG. Studies on the Circulation. II. Cardiac output determinations: Comparison of the injection procedure with the direct Fick method. Am J Physiol. 1929; 89:331.
2. Coulam CM, Warner HR, Wood EH, Bassingthwaighte JB. A transfer function analysis of coronary and renal circulation calculated from upstream and downstream indicator dilution curves. Circulation Res. 1966; 19:879. [PubMed: 5333498]
3. Zierler, KL. Handbook of Physiology: Circulation. Vol. 1. American Physiological Society; Washington, D.C.: 1962. Circulation times and the theory of indicator-dilution methods for determining blood flow and volume; p. 585-615.Section 2
4. Nicholes KRK, Warner HR, Wood EH. A study of the dispersion of an indicator in the circulation. Ann NY Acad Sci. 1964; 115:721. [PubMed: 14214047]
5. Gibson, JE. Nonlinear Automatic Control. McGraw-Hill; New York: 1963. p. 1-4.

6. Birkhead NC, Fox IJ, Wood EH. Effect of doubling and quadrupling indicator dose on dilution curves. The Physiologist. 1957; 1:11. Abstract.
7. Lee, YW. Statistical Theory of Communication. Wiley; New York: 1961. p. 5
8. Hamming, RW. Numerical Methods for Scientists and Engineers. McGraw-Hill; New York: 1962. p. 276-280.
9. Caro CG. The dispersion of indicator flowing through simplified models of the circulation and its relevance to velocity profile in blood vessels. British J Physiol. 1966; 185:501.

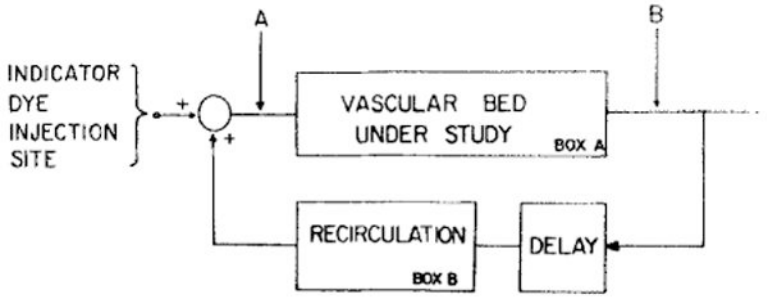

Fig. 1.

A simplified model of the circulatory system. The forward loop represents the vascular bed whose transfer function is to be found. The feedback loop represents a lumped vascular bed which accounts for the recirculation. A is the upstream sampling site; B, the downstream sampling site.

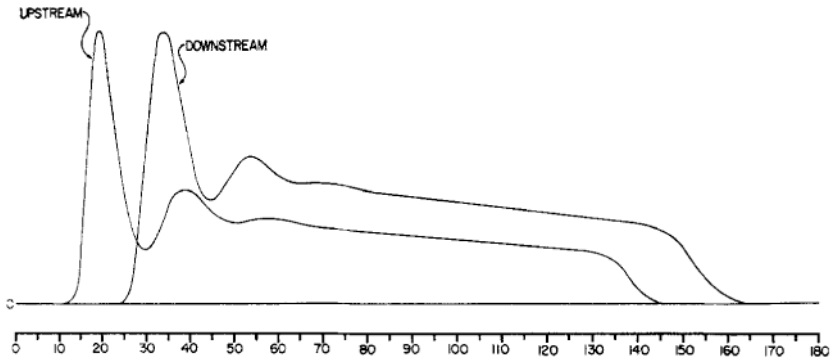

Fig. 2.

A terminated upstream and downstream indicator—dilution curve representation found by using Eq. (9)–(14). For these curves $\sigma = P/30$; $t_0 = P/12$, and $\tau = 2$. The abscissa has units of time; the ordinate, concentration.

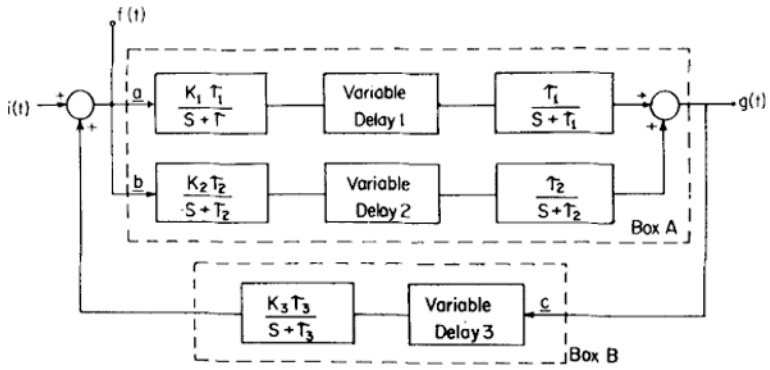

Fig. 3.

A model of a three-pathway circulatory mixing process which can be programmed on the analog computer. Each parallel pathway is represented by a gain factor K, a break frequency term τ, and a delay time.

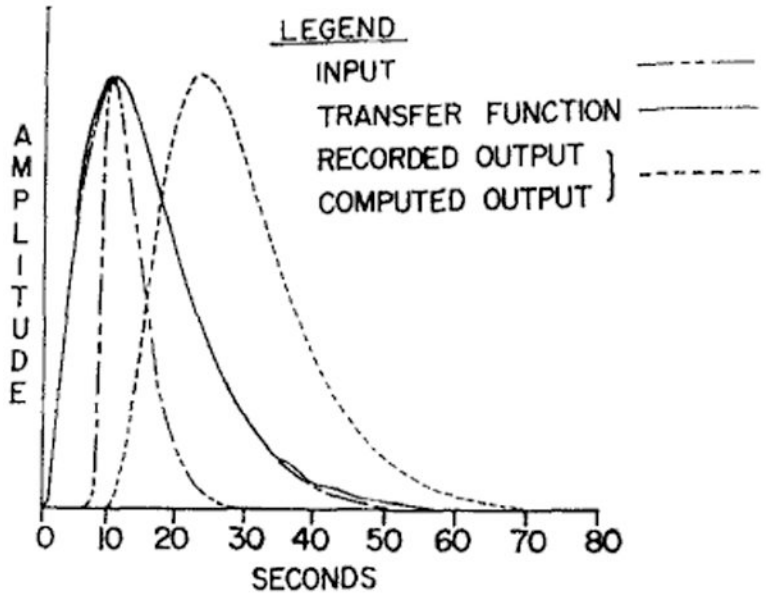

Fig. 4.

A recording of an input curve, output curve, and impulse response of the model of Fig. 3. For these curves $K_1 = 1$, $K_2 = K_3 = 0$; $\tau_1 = 2$; and delay time = 8 sec. Also shown are the computed impulse response and the computed downstream curve. Correlation between computed and recorded downstream curves is 0.9999. Sampling rate is six samples/sec.

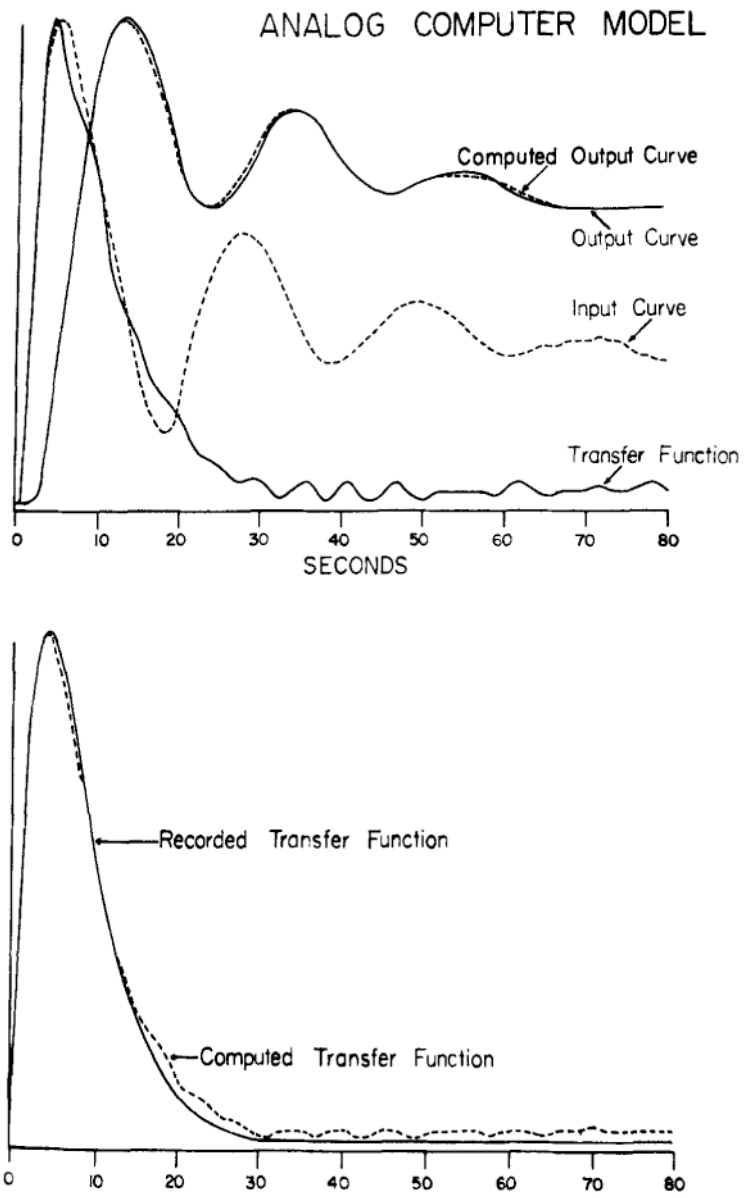

Fig. 5.

A recording of the input, output, computed output, and computed transfer function of the model of Fig. 3 is found in the upper frame. The lower frame shows the superposition of the recorded and computed impulse responses. Correlation between recorded and computed output curves is 0.999. $K_1 = K_3 = 1$, $K_2 = 0$; $\tau_1 = 4$, $\tau_3 = 1$; delay 1=0, delay 3 = 3 sec. Sampling rate is six samples/sec.

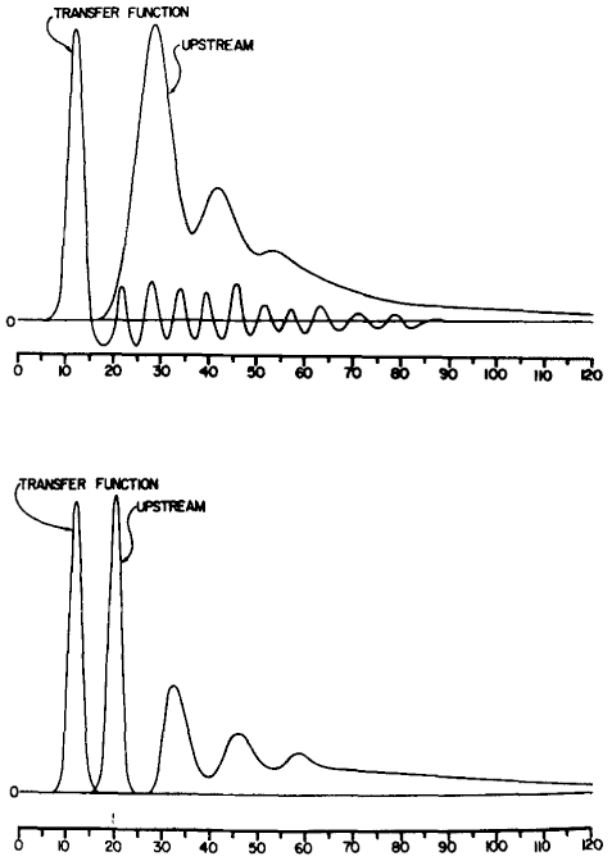

Fig. 6.

The upper frame shows the computed impulse response and input curve (with feedback) of the model of Fig. 3, where the input curve contained a harmonic bandwidth less than that of the transfer function. The lower frame shows where both input and computed transfer function contain the same harmonic content.

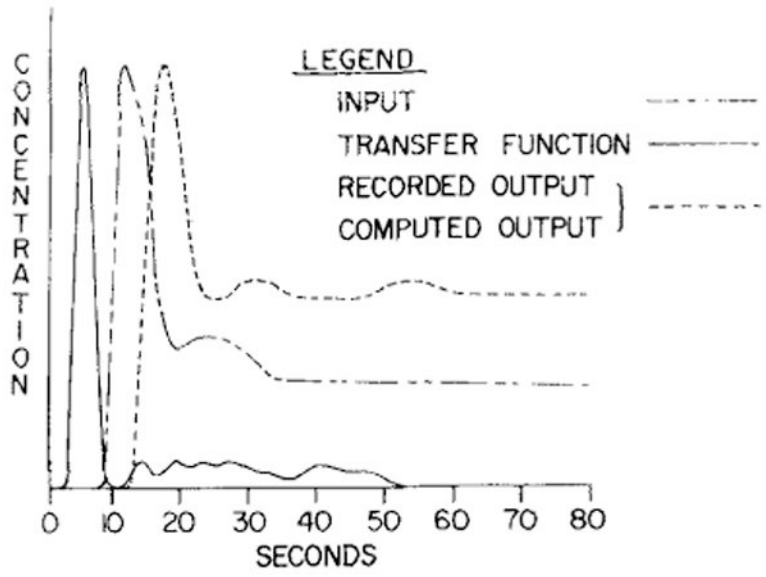

Fig. 7.

The effects of aliasing on the transfer-function computation are shown here. Represented are the input curve, output curve, computed output curve, and computed transfer function. A 20-Hz signal ($S/N = 10$) was added to the input and output curves; the sampling rate was six samples/sec. Correlation between input and output curves is 0.85.

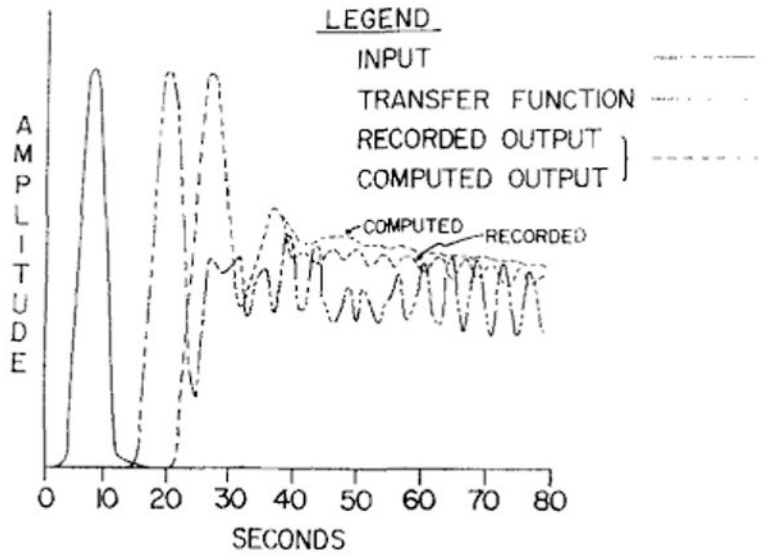

Fig. 8.

A representation of an upstream curve (aortic arch), downstream curve (renal vein), computed downstream curve (correlation = 0.998), and computed renal transfer function found from an anesthetized dog (Nembutal, 30 mg/Kg.

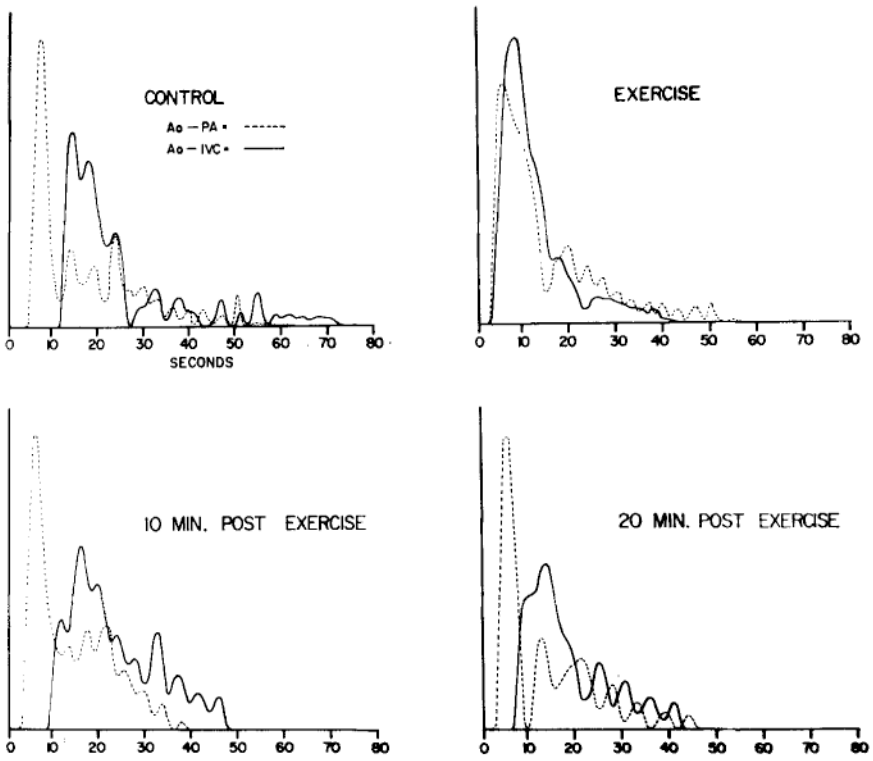

Fig. 9.

A four-frame representation of the systemic and lower-extremity blood-distribution patterns of a dog that occur before (upper left), during (upper right), and following (lower) moderate exercise (walking at two miles per hour for four min). Note the change in distibution patterns during the exercise state.